Journal of Materials Chemistry B

Accepted Manuscript

ROYAL SOCIETY OF CHEMISTRY

www.rsc.org/materialsB

Journal of Materials Chemistry B

ARTICLE

Evaluation of enzymatically crosslinked injectable glycol chitosan hydrogel

Received 00th January 20xx,
Accepted 00th January 20xx

DOI: 10.1039/x0xx00000x

www.rsc.org/

Shalini V Gohil,[a,b,#] Sarah B Brittain,[c,#] Ho-Man Kan,[a,b] Hicham M Drissi,[a] David W Rowe,[d] and Lakshmi S Nair*[a,b,c,e]

Enzymatically cross-linkable phenol-conjugated glycol chitosan was prepared by reacting glycol chitosan with 3-(4-hydroxyphenyl) propionic acid (HPP). The chemical modification was confirmed by FTIR, 1H-NMR and UV spectroscopy. Glycol chitosan hydrogels (HPP-GC) with or without rhBMP-2 were prepared by the oxidative coupling of the substituted phenol groups in the presence of hydrogen peroxide and horse radish peroxidase. Rheological characterization demonstrated the feasibility of developing hydrogels with varying storage moduli by changing the polymer concentration. The gel presented a microporous structure with pore sizes ranging from 50-350 µm. The good viability of encapsulated 7F2 osteoblasts indicated non-toxicity of the gelation conditions. In vitro release of rhBMP-2 in phosphate buffer solution showed ~11% release in 360 h. The ability of the hydrogel to maintain the *in vivo* bioactivity of rhBMP-2 was evaluated in a bilateral critical size calvarial bone defect model in Col3.6 transgenic fluorescent reporter mice. The presence of fluorescent green osteoblast cells with overlying red alizarin complexone and yellow stain indicating osteoclast TRAP activity confirmed active cell-mediated mineralization and remodelling process at the implantation site. The complete closure of the defect site at 4 and 8 weeks post implantation demonstrated the potent osteoinductivity of the rhBMP-2 containing gel.

1. Introduction

Hydrogels are highly hydrated three-dimensional (3-D) networks composed of cross-linked hydrophilic polymers and have been extensively studied for a variety of biomedical and biopharmaceutical applications.[1-3] The unique, tissue-mimetic properties of the hydrogels, excellent gas/nutrient diffusion and high porosity make them particularly useful for regenerative engineering as a cell/protein delivery system.[4-7] Injectable hydrogels are especially desirable clinically, to achieve uniform distribution of cells and proteins within the gel and due to the potential for minimally invasive delivery using endoscopic or percutaneous procedures.[8, 9] Injectable hydrogels can be developed using various external stimuli including light (photo-polymerizing/photo-gelling systems), chemical agents (chemical and ionic crosslinking systems) and physiological factors (temperature, pH and ionic strength).[4] Recently, enzyme catalyzed reactions have emerged as a novel approach to develop injectable hydrogels due to its high specificity and ability to work under physiological conditions (aqueous, pH 6-8, 37°C) without unwanted side reactions or cytotoxicity.[10-12]

Transglutaminase, peroxidase, tyraminase, laccase, lysyl oxidase, phosphatase and metalloproteinases are some of the currently investigated enzyme systems for *in situ* hydrogel formation.[10-12] Among these, enzyme catalyzed crosslinking of polymers using peroxidases such as horse radish peroxidase (HRP) is one of the most extensively investigated approaches.[13-17] Both natural and synthetic polymers containing phenol groups or those functionalized with tyramine, tyrosine or other aminophenol molecules can be cross-linked effectively using peroxidases.[18] Briefly, in the presence of hydrogen peroxide (H_2O_2) and HRP, the phenolic groups in the polymers undergo one-electron oxidation and generate reactive radical groups which subsequently react with each other to form the cross-linked hydrogel.[17, 19] The *in vitro* and *in vivo* biocompatibility of peroxidase cross-linked

[a] Department of Orthopaedic Surgery, UConn Health, Farmington, Connecticut, US 06030
[b] Institute for Regenerative Engineering, The Raymond Beverly Sackler Center for Biomedical, Biological, Physical and Engineering Sciences, UConn Health, Farmington, Connecticut, US 06030
[c] Department of Biomedical Engineering, University of Connecticut, Storrs, Connecticut, US 06269
[d] Center for Regenerative Medicine and Skeletal Development, Department of Reconstructive Sciences, School of Dental Medicine, UConn Health, Farmington, Connecticut, US 06030
[e] Departments of Material Science and Engineering, Institute of Material Science, University of Connecticut, Storrs, Connecticut, US 06269
[#] Equal First Authorship; *Corresponding Author
Corresponding author's address: Lakshmi S. Nair, M.Phil. PhD, Assistant Professor; Department of Orthopedic Surgery, UConn Health; E-7041, MC-3711; 263 Farmington Avenue, Farmington, CT-06030; E mail: nair@uchc.edu

hydrogels has been demonstrated using a wide range of polymers.[4, 13, 17, 20-22]

Chitosan is a natural, hydrophilic, polysaccharide extensively studied as a biomaterial due to its non-toxic, biocompatible and biodegradable properties.[23-25] It is a linear co-polymer consisting of ß(1-4)-linked glucosamine units and N-acetyl glucosamine units.[26] Chitosan is derived from chitin, the second most abundant natural polymer and is isolated from the exoskeleton of crustaceans including crab, shrimp and lobster. Chitosan, therefore raises considerable attention as a potential biomaterial for musculoskeletal tissue engineering and has been used to develop sponges, hydrogels and composite matrices.[26-28] The cationic amino groups on the C2 position of the glucopyranose units of chitosan can facilitate the formation of ionic complexes with a variety of anionic molecules.[29, 30] This property, along with its mucoadhesive nature and ease of chemical functionalization makes chitosan one of the most extensively studied polymers for protein and drug delivery applications.[31, 32]

Sakai *et al* previously reported an enzymatically cross-linkable chitosan hydrogel for *in situ* local delivery.[33] Due to the limited solubility of chitosan at physiological pH, complete dissolution of the chitosan could be obtained only at a pH of 3.5, and the solution pH needed to be later adjusted to 7 using sodium hydroxide. The need for acidic pH for polymer dissolution may limit the use of chitosan as injectable hydrogel for protein and cell delivery applications.[34] Another study investigated the feasibility of increasing the water solubility of chitosan by grafting glycolic acid (GA). The potential of enzymatically cross-linked phloretic acid substituted and GA grafted chitosan as an injectable hydrogel for cartilage tissue engineering has been demonstrated.[35]

A number of methods including PEGylation, carboxymethylation, reductive amination with phosphorylcholine–glyceraldehyde, as well as attaching hydrophilic groups such as acrylic acid have been investigated to improve the water solubility of chitosan.[36, 37] Glycol chitosan is a chitosan derivative with a glycol moiety at C6 hydroxyl group, that makes it completely water soluble and also maintains the desirable properties of chitosan as a biomaterial.[38] The highly reactive amino groups of glycol chitosan also allows for chemical modification without adversely affecting the aqueous solubility.[39-42] Glycol chitosan has been extensively investigated in the form of micro and nanoparticles for drug delivery applications.[43, 44] Photopolymerizable methacrylated glycol chitosan has been recently developed as a biomaterial.[45, 46] The feasibility of developing *in situ* cross-linkable glycol chitosan gels using multi-benzaldehyde functionalized PEG analogues has also been demonstrated.[47]

In this study, the potential of developing an injectable glycol chitosan hydrogel using peroxidase mediated enzymatic reaction was investigated. Phenolic groups were incorporated in glycol chitosan by reacting it with hydroxyphenyl propionic acid (HPP) using standard carbodiimide chemistry and the modified polymer was characterized by attenuated total reflectance-Fourier transform infrared (ATR-FTIR) and proton nuclear magnetic resonance (^{1}H-NMR) spectroscopy. The morphology, rheological behaviour, cytocompatibility as well as protein release from the enzymatically cross-linked hydrogel were evaluated. The potential of the gel to retain the biological activity of encapsulated protein was evaluated *in vivo* using a bilateral, calvarial bone defect in transgenic fluorescent reporter mice using recombinant bone morphogenetic protein-2 (rhBMP-2).

2. Materials and methods

2.1. Materials

Glycol-chitosan (≥60% (titration), crystalline) and morpholinoethanesulfonic acid (MES) solution (1M, BioReagent, for molecular biology, suitable for cell culture) were purchased from Sigma. N-3-dimethylaminopropyl-N-ethyl carbodiimide hydrochloride (EDC), N-hydroxysuccinimide (98%) (NHS), 3-(4-Hydroxyphenyl) propionic acid (98%) (HPP), H_2O_2 and HRP were purchased from Sigma Aldrich. Chinese hamster ovary (CHO) cell-derived recombinant human bone morphogenetic protein-2 (rhBMP-2) and rhBMP-2 enzyme-linked immunosorbent assay (ELISA) kit were obtained from R&D Systems. Deuterium oxide "100%" (D, 99.96%) +0.01 MG/ML DSS was obtained from Cambridge Isotope Laboratories, Inc. LIVE/DEAD® Viability/Cytotoxicity Kit (for mammalian cells) was obtained from Life Technologies. All other chemicals used were of reagent grade and obtained from Fisher Scientific.

2.2. Preparation of HPP-modified glycol-chitosan

Glycol chitosan was chemically modified with HPP using an aqueous carbodiimide coupling reaction. Briefly, 500 mg of glycol chitosan was dissolved in 350 mL of 1 M MES solution (pH 5.5) for 3 h at room temperature. EDC (2.608 mmol) and NHS (2.172 mmol) were dissolved in 50 mL of MES solution and allowed to react with HPP (3.009 mmol) for 1 h. This solution was then added to the glycol chitosan solution and allowed to react for 24 h at room temperature. The reaction mixture was dialyzed against water for 3 days (with at least 6 changes of water) using dialysis tubing with 10,000 Da molecular weight cut-off, to remove the excess reactants (EDC, NHS and HPP) as well as the by-products. The resulting HPP modified glycol chitosan (HPP-GC) was lyophilized and stored at -20°C until further use.

2.3. Characterization of HPP-modified glycol-chitosan

ATR-FTIR, ^{1}H-NMR and UV spectroscopy were utilized to confirm the presence of phenol groups in HPP-GC. Briefly, ATR-FTIR spectra was obtained over 200 scans using Nicolet iS10 spectrometer (Thermo Scientific) equipped with a SMART iTR accessory, in the 650-4000 cm^{-1} region. The spectrum of glycol chitosan was subtracted from that of HPP-GC using Omnic 8.0 software (Thermo Scientific) to identify the new peaks arising from phenol modification. For ^{1}H-NMR, 5 mg samples were dissolved in 0.5 ml deuterium oxide and analyzed using a 800 MHz Agilent VNMRS spectrometer equipped with a triple resonance HCN cold probe. The ^{1}H-NMR spectra for each sample were collected at 68°C with 8,992.8 Hz bandwidth, 32K

complex data points, 128 transients, a flip angle of 90°, and a 40 second recycle delay to ensure complete relaxation for proper integrations. All spectra were processed and analysed using Mnova software from Mestrelab Research, Santiago de Compostela, Spain. The phenolic content of resulting HPP-GC polymer was quantified using UV-Visible Spectrophotometer (UV-Mini-1240; Shimadzu). The glycol chitosan and HPP-GC samples were dissolved in ultra-pure water and the absorbance was measured at 275 nm. Phenolic substitution was calculated from a standard curve prepared using various concentrations of HPP dissolved in ultra-pure water.

2.4. Enzymatic crosslinking of HPP-modified glycol chitosan

HPP-GC was dissolved in a 1:1 v/v solution of ultrapure water and α-MEM media at various concentrations. HRP was then added to the HPP-GC solution to obtain a concentration of 20 units per ml. Enzymatic cross-linking was initiated *via* addition of H_2O_2 in HPP-GC-HRP solution to give a final H_2O_2 concentration of 7.349 mM.

2.5. Characterization of HPP-modified glycol chitosan hydrogels

Morphology of the HPP-GC hydrogels was determined using JEOL 6335 Field Emission Scanning Electron Microscope (SEM) operated at an accelerating voltage of 10 kV and 12 µA. Briefly, 15 µl of HPP-GC was used to prepare the hydrogel on aluminum stubs, flash frozen in liquid nitrogen and then freeze-dried. Prior to imaging, the samples were platinum coated for improved conductivity.

The rheological properties of the HPP-GC hydrogels were evaluated on Discovery HR3 hybrid Rheometer (TA Instruments), using 12 mm parallel plate geometry. Various concentrations (0.5, 1, 2 and 4% w/v) of HPP-GC polymer solutions were prepared. All measurements were performed in the linear viscoelastic range. The gels were prepared as discussed in section 2.4. Briefly, 110 µl of HPP-GC solution containing HRP was conditioned (pre-shear rate: 50 rad/s; time: 10 s; gap width: 1000 µm) at 37°C, during which gelation was induced by quick addition of H_2O_2 solution, using "Gel-Saver" gel loading pipet tips (USA Scientific). The samples were then equilibrated at 37°C for 60 s to ensure complete gelation. Dynamic logarithmic frequency sweeps from 0.1 to 100 rad/s at a strain of 10% were then performed to evaluate the rheological properties of HPP-GC gels at various concentrations.

2.6. Cytocompatibility of HPP-modified glycol chitosan hydrogel

Briefly, mouse bone marrow derived osteoblast cell line 7F2 (ATCC® CRL-12557™) were cultured in alpha minimum essential medium containing 2 mM l-glutamine and 1 mM sodium pyruvate without ribonucleosides and deoxyribonucleosides, 10% fetal bovine serum, and 1% penicillin-streptomycin. Cells were suspended in HPP-GC solution containing HRP at a seeding density of 0.5 million per ml, and H_2O_2 was then added to obtain a final concentration of 7.349 mM, to induce gelation. After predetermined time of incubation at 37°C and 5% CO_2, the cells were stained with LIVE/DEAD® Viability/Cytotoxicity Kit and imaged using confocal microscopy (Zeiss LSM 510 Meta, USA).

2.7. *In vitro* protein release from HPP-modified glycol chitosan hydrogel

rhBMP-2 solution (1 µg/µl in sterile 4 mM HCl) was added to 2% w/v HPP-GC polymer-HRP solution. The gels were fabricated in the form of discs using a mold to ensure uniform gel dimensions across samples. The rhBMP-2-HPP-GC-HRP solution was added to the mold and gelation was induced by the addition of H_2O_2, as discussed in section 2.4. The discs (15µl gel solution containing 2 µg rhBMP-2 per disc, n = 4) were incubated in 400 µl phosphate buffer solution (PBS) at 37°C with gentle rocking. At each time point, 200 µl of the release medium was removed and replaced with an equal amount of PBS. The rhBMP-2 released at each time point was quantified using rhBMP-2 ELISA kit, at 450 nm with 540 nm as the reference wave length, as per manufacturer instructions.

2.8. *In vivo* repair of critical sized bone defects

The experimental protocol was approved by the institutional animal care committee, UConn Health. CD-1 transgenic mice containing the 3.6-kb fragment of the rat collagen type 1 promoter driving the expression of a EYFP topaz-fluorescent protein (Col3.6Tpz; EYFP; green), constructed in the laboratory of David Rowe at UConn Health, were used in the study (n=8, average age: 10 weeks). The transgenic mice used in this study were generated, bred and maintained at the Center for Laboratory Animal Care of UConn Health. The animals had free access to both sterile water and standard rodent chow ad libitum. Briefly, the mice were anesthetized with Ketamine (135 mg/kg)/Xylazine (15 mg/kg) combination (I.P). The head was shaved and the surgical site was cleaned with 75% ethanol. An incision was made just off the sagittal midline to expose the parietal bone. On both sides of non-suture associated parietal bone, 3.5 mm defects were made using a trephine drill. The calvarial disk was removed carefully in order to avoid injury to the underlying dura mater. One of the defects was implanted with rhBMP-2 loaded hydrogel (HPP-GC+BMP) (2µg rhBMP-2) and the neighbouring defect was implanted with HPP-GC hydrogel alone (HPP-GC). The skin was sutured with 5-0 vicryl followed by subcutaneous injection of buprenorphine (0.08 mg/ kg) for analgesia. An additional dose of buprenorphine was given within 24 h of surgery. The mice were injected with alizarin complexone (AC) (30 mg/Kg body weight, I.P.), one day before sacrifice.

At 4 and 8 weeks post-surgery, the animals (n=4 at each time point) were sacrificed by CO_2 asphyxiation followed by cervical dislocation. Calvaria were dissected from the skull and fixed in 10% formalin for four days. The calvaria were then transferred into a 30% sucrose solution in PBS, pH 7.4 for one day. The tissue was then positioned in Shandon Cryomatrix™, frozen on dry ice and stored in air tight plastic bags at -20°C until sectioning. Cryosections (5 µm) through the non-decalcified calvaria were obtained on a Leica CM3050S cryostat (Leica, Wetzlar) using a disposable steel blade (Thermo Scientific) and tape transfer process (Cryofilm type IIC (10), Section-Lab Co. Ltd.). The cryosections were then sequentially imaged by darkfield imaging, alkaline phosphatase

(ALP) staining, tartrate-resistant acid phosphatase (TRAP) staining and hematoxylin counterstaining.

2.9. Statistical analysis

The results of quantification are expressed as mean ± standard deviation. Statistical analysis was performed using SigmaStat Version 2.3. Statistically significant values were defined as $p < 0.05$, based on one way ANOVA followed by Student's Newman-Keuls test.

3. Results and Discussion

3.1. Synthesis and characterization of enzymatically cross-linked chitosan gel

As a first step to develop injectable chitosan gels that can be gelled under physiological conditions, phenol groups were introduced in glycol chitosan. The modification involved initial activation of carboxyl groups of HPP by EDC to form an active O-acylisourea intermediate, which can subsequently react with the primary amino groups of glycol chitosan (Fig. 1A).

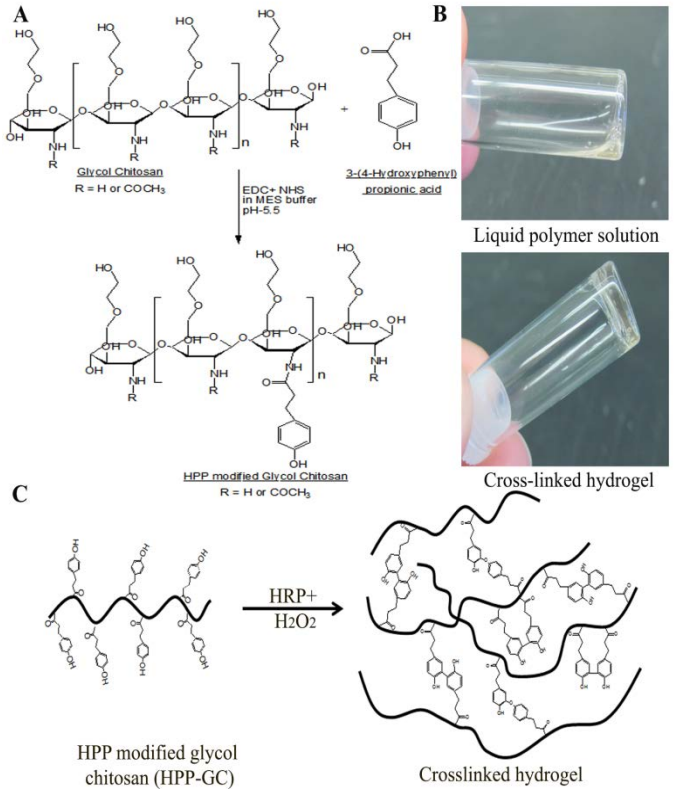

Fig. 1 A) Schematic showing the HPP modification of glycol chitosan using carbodiimide mediated coupling B) Photograph showing HPP-GC polymer solution in 50:50 water:α-MEM and the corresponding hydrogel after enzymatic cross-linking using HRP and H_2O_2 C) Graphical representation of the enzymatic cross-linking process resulting in the formation of HPP-GC hydrogel

The HPP-GC obtained by phenol modification of glycol chitosan was fluffy, white coloured solid. The spectral subtraction of glycol chitosan from HPP-GC showed the presence of new peaks of amide C=O (1629 cm^{-1}), aromatic C=C (1517.3 cm^{-1}) and CH bends (765.4 cm^{-1}), p-substituted aromatic group (865.6 cm^{-1}), phenol OH bend (1307.7 cm^{-1}) and the peaks corresponding to C-O stretch for phenol/ether group (1032.5, 1172.9 and 1106.1cm^{-1}) (Fig. 2A) indicating the incorporation of phenol moiety in the HPP-GC polymer. ^{1}H-NMR of HPP-GC showed characteristic peaks for aromatic protons between 6.8 and 7.2 ppm, located outside of the generic chitosan spectra (Fig. 2B). The appearance of new peaks corresponding to aromatic protons confirmed the successful incorporation of phenol groups in the HPP-GC polymer. Quantification of phenol content by UV spectroscopy showed 0.377 ± 0.061 µmoles of phenol groups per mg of HPP-GC. Unlike previously reported phenol derivative of chitosan, due to the high aqueous solubility of glycol chitosan, the resulting HPP-GC was highly soluble in aqueous media at physiological pH.[33] This may provide significant advantages as an injectable cell/protein/growth factor delivery vehicle due to the potential to maintain good cell viability and protein bioactivity.

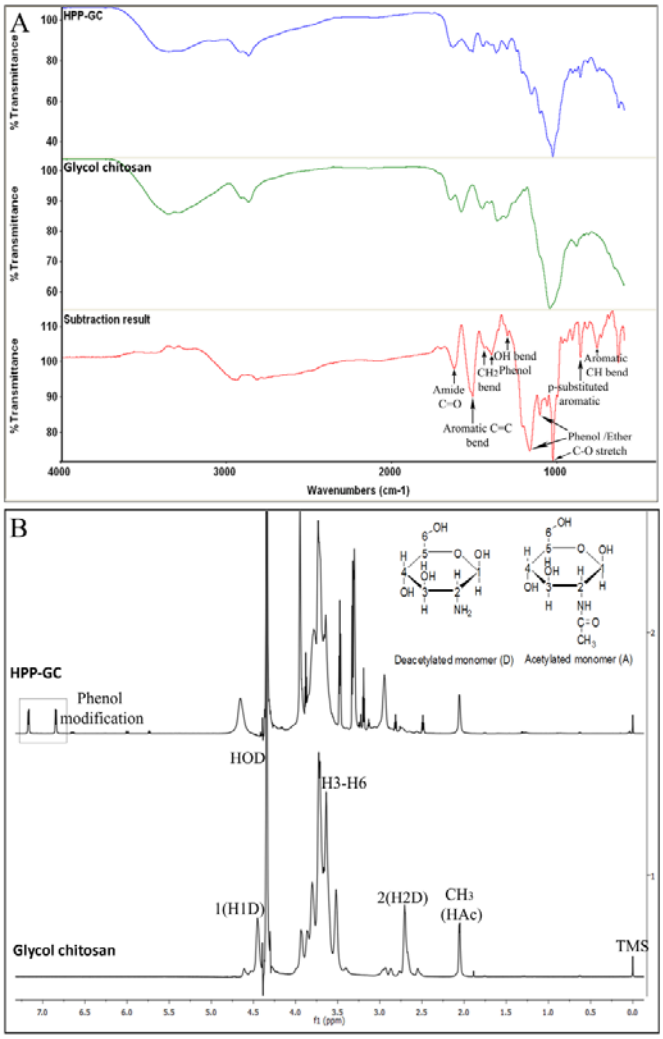

Fig. 2 Characterization of HPP-GC polymer using A) ATR-FTIR B) ^{1}H NMR showing characteristic peaks upon HPP modification of glycol chitosan. Trimethyl silane (TMS) was used as the reference. HOD refers to the peak for deuterium oxide. The protons specific to chitosan are also labelled.

Fig. 1B shows the conversion of liquid HPP-GC into a non-flowing, solid gel in the presence of HRP and H_2O_2. The process involves reaction of H_2O_2 to the heme group at the active site

of HRP enzyme leading to the formation of an oxoferryl centre and a porphyrin-based cation radical. This complex serves as a reducing agent and undergoes oxidation in the presence of phenolic oxidizing agent. Subsequently, the two phenolic radical species react to form covalent crosslinks.[48] The cross-linking may occur through either C–C bonds between ortho-carbons of the aromatic ring or through C–O bonds between ortho-carbon and phenolic oxygen [17, 49], as shown in Fig. 1C. Irrespective of the polymer concentration (0.5, 1, 2 and 4% w/v), the gelation time of HPP-GC solutions was less than 1 minute. The fast gelation observed in this system may be advantageous to prevent undesirable diffusion of hydrogel precursors as well as loaded bioactive molecules from the injection site.[50]

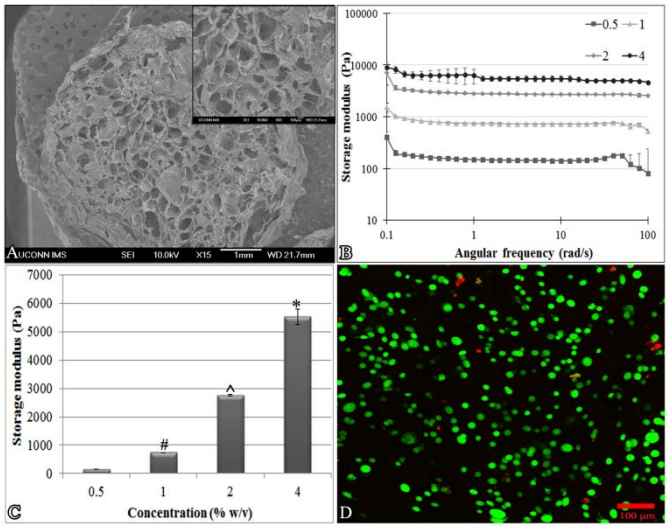

Fig. 3 A) Morphology of enzymatically cross-linked HPP-GC hydrogels [Magnification: 15X and 50X (inset)] B) Dynamic rheological characterization of HPP-GC hydrogels of different polymer concentrations showing frequency dependence of storage modulus C) Average storage modulus of the hydrogels as a function of polymer concentration D) Z-stacked confocal image showing viability of 7F2 osteoblasts after 3h of *in situ* gelation. Data is expressed as mean ± standard deviation, n=4. One way ANOVA followed by Student's Newman-Keuls test; p*<0.001 Vs 0.5, 1, 2% w/v, p^<0.001 Vs 0.5, 1% w/v, p#<0.001 Vs 0.5% w/v

The morphology of the hydrogel (2% w/v) was evaluated by SEM and showed an interconnected porous microstructure with micro-pores ranging from 50-350 µm (Fig. 3A). Lyophilized chitosan sponge has shown to have an open porous structure and parameters such as freezing temperature and polymer concentration may affect the pore diameter.[51] The pore structure of the enzymatically cross-linked HPP-GC hydrogel in the present study was found to be comparable to that formed by photocrosslinking as well as by PEG-benzaldehyde or PEO-PPO-PEO-benzaldehyde crosslinking of glycol chitosan.[45, 47] The porous interior morphology of the hydrogel is advantageous for cell encapsulation to facilitate the migration of encapsulated cells as well as support nutrient and gaseous diffusion. Further, the rheological behaviour of the hydrogels was evaluated as a function of polymer concentration. Fig. 3B&C show frequency dependence and the storage moduli of hydrogels prepared from 0.5, 1, 2 and 4% w/v HPP-GC polymer, respectively. In the tested frequency range, the storage modulus was found to be independent of frequency indicating the stability of the crosslinked hydrogels.[52] Further, the storage modulus was found to significantly increase with increasing polymer concentrations. The 0.5 % gels showed a lower modulus of about 145±2 Pa compared to the 2% and 4% gels with modulus of 2756±35 Pa and 5520±269 Pa respectively. Previous studies have shown that photo cross-linking 2% glycol chitosan solution resulted in gels with modules of ~1800Pa.[45] Similarly, crosslinking 1.5% glycol chitosan solution with various concentrations of benzaldehyde functionalized PEG analogues resulted in gels with storage modulus ranging from 210-1400 Pa.[47] In another study, crosslinking of 5% glycol chitosan with benzaldehyde-capped PEO-PPO-PEO showed the feasibility to develop gels with modulus greater than 3000 Pa, depending on the benzaldehyde-capped PEO-PPO-PEO concentration.[52] The present data demonstrates the feasibility to develop stable glycol chitosan gels using an enzymatic process and that the gel modulus can be significantly varied by varying the polymer concentration. Since substrate stiffness can have significant effect on encapsulated cellular functions, the feasibility to modulate gel stiffness will be advantageous for fine-tuning the substrate properties for cell delivery applications.[17, 53]

Even though enzymatic crosslinking has been used to develop hydrogels from many polymers, the studies have used a wide range of HRP and H_2O_2 concentrations.[13, 54, 55] In the present study 20 units per ml HRP and 7.35 mM H_2O_2 was used to initiate crosslinking. In order to confirm the non-toxicity of the crosslinking conditions, the cytocompatibility of the enzymatically cross-linked glycol chitosan was evaluated by encapsulating 7F2 osteoblast cells in the gels under the standard gelation conditions (Fig. 3D). More than 97% of the encapsulated cells were viable after 3 h of encapsulation, as evidenced from the green fluorescence, demonstrating the non-toxicity of the gelation conditions. The encapsulated 7F2 cells did not show any significant reduction in % cell viability, even after 7 days of culture (Supplementary figure S1).

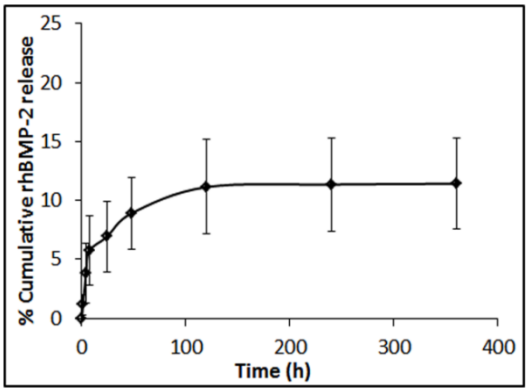

Fig. 4 Cumulative percent release of rhBMP-2 from HPP-GC hydrogel

3.2. *In vitro* rhBMP-2 release

The potential of the injectable HPP-GC gel to serve as a protein delivery vehicle was evaluated *in vitro* by following the release of rhBMP-2 from the gels as a function of time (Fig. 4). The hydrogel maintained its 3-D structure without disintegration or

dissolution during the study. rhBMP-2 showed a burst release of approximately 9% in the first 48 h. An additional release of about 2% was observed until 120 h. No significant release was observed afterwards indicating that the rest of the encapsulated protein was retained within the gel.

Chitosan based hydrogels have been extensively investigated to deliver small and macro-molecules for a wide range of applications. Li *et al* recently evaluated the potential of a thermoresponsive glycol chitin hydrogel as a delivery vehicle for doxorubicin (DOX).[41] The gel showed an initial burst release of ~20%, followed by a diffusion controlled sustained release of >80%, over a period of 13 days. On the other hand, hydrogels prepared by *in situ* crosslinking of glycol chitosan with benzaldehyde-capped PEO-PPO-PEO could only release 30% of loaded DOX after 150 h of incubation.[52] The lower drug release in this study was attributed to potential additional hydrogen bonding interactions of the DOX molecule with the polymer matrix as well as due to the possible reaction of amino groups of DOX with the polymeric aldehyde groups, resulting in chemical conjugation of the drug to the gel matrix. Similarly, the possibility of chitosan matrix to interact with encapsulated proteins was demonstrated using a thermosensitive quaternized chitosan PEG gel.[56] The release profile of insulin from the gel showed a burst release followed by slower release and the release rate depended on the molecular weight and concentration of PEG as well as on insulin concentration. The low protein release from the matrix was attributed to the hydrogen bonding of amino groups and hydroxy groups of insulin molecule with PEG or quaternized chitosan.

Another study investigated the release of insulin and bovine serum albumin (BSA) from disulphide cross-linked chitosan hydrogel.[57] Unlike the quaternized hydrogel, disulphide cross-linked chitosan gel showed a faster release with more than 60% protein release in the first 72 h. However, 100% release of encapsulated protein could not be observed indicating the presence of hydrogen bonding and hydrophobic interactions between protein and the gel as well as possible chemical reaction of the protein with the thiol group of gel precursors. Bae *et al* recently investigated the potential of disulfide cross-linked chitosan hydrogel as rhBMP-2 delivery vehicle.[58] The rh-BMP-2 encapsulated in chitosan gel showed ~70% release within 7 days, showing the feasibility of chitosan gel to support sustained rhBMP-2 release.

In addition, the enzymatic crosslinking conditions may also significantly affect protein release from the gels. In HRP mediated enzymatic crosslinking, the concentration of HRP and H_2O_2 has shown to significantly affect the gel properties. The effect of H_2O_2 concentration on the extent of gel crosslinking as well as the swelling ratio has been demonstrated using tyraminated hyaluronic acid (HA) hydrogels.[21, 59] Using a model protein lysozyme, it has been shown that gels prepared with low H_2O_2 concentration showed ~60% release in 24 h whereas, only 15% release was observed from gels prepared with high H_2O_2 concentration. These studies indicate the potential of gel-protein interactions as well the enzymatic gelation conditions to modulate the protein release from the hydrogels.

In the present study, rhBMP-2 (Isoelectric point = 8.5) showed a small burst release followed by almost complete retention of the protein in the glycol chitosan gel (~90%). The effect of HRP and H_2O_2 concentrations on the physical and mechanical properties of phenolated glycol chitosan is not known. Further studies are required to systematically understand the effect of reagent concentrations on hydrogel properties and its subsequent effect on protein release. Since rhBMP-2 has tyrosine groups, the use of higher HRP and H_2O_2 concentrations in the present study raises the possibility of rhBMP-2 forming chemical bonds with the chitosan matrix. Studies are currently underway to understand the extent of chemical binding and delineate its effect from physical interaction of the matrix with encapsulated protein.

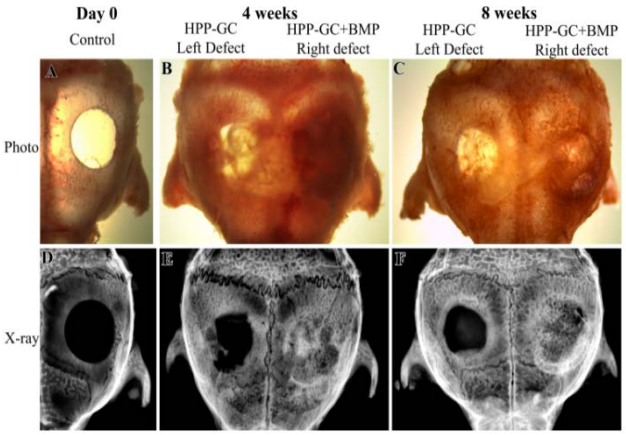

Fig. 5 Representative images of isolated calvaria showing whole calvaia and X-ray images of control group at day 0 (A, D) and groups implanted with enzymatically cross-linked, injectable HPP-GC hydrogels with and without rhBMP-2 at 4 weeks (B, E) and 8 weeks (C,F) post-implantation

Previous studies have shown that direct injection of rhBMP-2 solution does not result in bone formation in the absence of a suitable carrier.[60] Clinical delivery of rhBMP-2, thus involves adsorption on a collagen sponge, which shows a burst release due to weak matrix-protein interactions.[61, 62] The burst release along with the supraphysiological doses used however, leads to side effects such as inflammation and ectopic bone formation.[63-66] One potential approach to overcome this limitation is covalent attachment of rhBMP-2 to the delivery system.[67, 68] Covalently attached growth factors may allow for prolonged signal transduction and protects the proteins from cellular internalization, inactivation and degradation.[69] Several reports have shown positive correlation between the retention of rhBMP-2 upon implantation and the osteoinductive activity, owing to its significantly short *in vivo* half-life ($t_{1/2}$ ~7-16 min).[70, 71] Various chemistries particularly carbodiimde and sulfo-SMCC have been studied to conjugate growth factors including rhBMP-2 to various biomaterials and the biological activity of the conjugated proteins.[72, 73] Depending on the immobilization chemistry, the covalent conjugation of a growth factor may lead to the loss of biological activity by inhibiting its binding to cell surface receptors. However, covalent conjugation of BMP-2 on chitosan films *via*

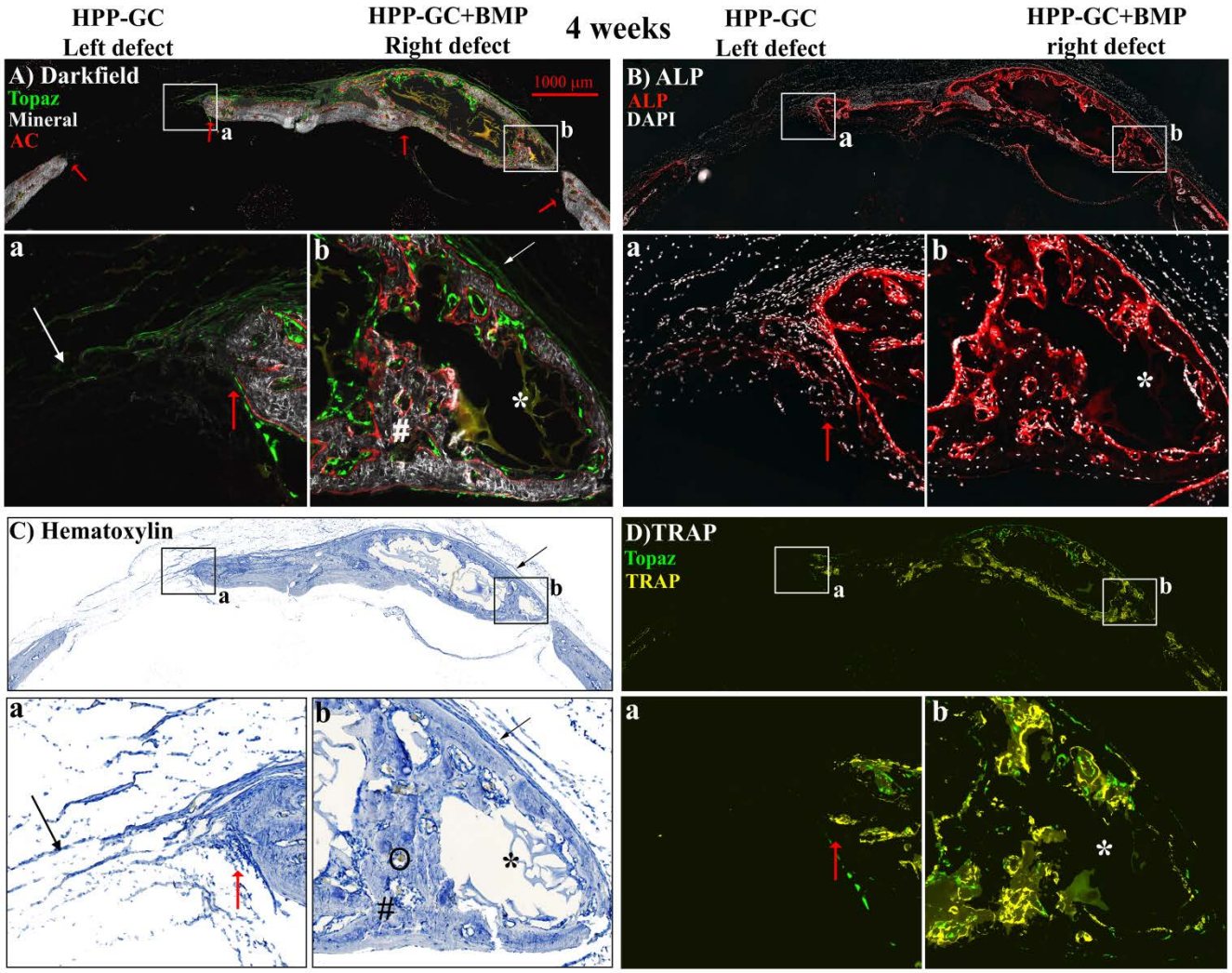

Fig. 6 Histology showing A) Darkfield, B) ALP, C) Hematoxylin and D) TRAP stained sections of the critical sized defects after 4 weeks of implantation with enzymatically cross-linked, injectable HPP-GC hydrogels with or without rhBMP-2. Full calvarial sections (scale bars: 1000 µm). Darkfield sections show EYFP reporter expression in the regenerated tissues along with alizarin complexone (AC) labelling. The defect edges are marked by red arrows. Bright, EYFP positive, green cells lined with a red mineralizing AC label are mature osteoblasts. Light green elongated cells form a periosteum-like layer at the periphery of the defects. TRAP: Bright yellow stain co-localized with low EYFP expressing cells represent TRAP positive osteoclasts. ALP: Red color indicates ALP positive cells. Cell nuclei are stained white with DAPI. (*) non-degraded gel; (#) New bone with embedded osteocytes; (circle) blood vessel; (arrow) Periosteum-like fibrous layer composed of cells expressing low EYFP, but negative for AC, ALP or TRAP

carbodiimide chemistry has been shown to result in higher retention (less than 20% release) as well as enhanced *in vitro* bioactivity and osteoblastic differentiation.[72] Furthermore, covalent crosslinking of alkaline phosphatase with a peptide tag containing tyrosine residues, *via* oxidative tyrosine coupling reaction in the presence of HRP and H_2O_2, showed ~95% retention of the native enzymatic activity.[74]

3.3 In vivo regeneration of critical sized calvarial defect

A preliminary *in vivo* study was therefore performed to evaluate if rhBMP-2 loaded injectable HPP-GG gel could induce bone formation in a critical sized defect model, although almost 90% of the encapsulated protein could not be released *in vitro*. Transgenic reporter mouse models present unique tools to understand the cellular processes during bone regeneration as well as delineate the biomaterial induced ectopic mineralization from active cell-mediated matrix deposition.[75] In the present study, a Col3.6 fluorescent reporter mouse with 3.6 kb Col1α1 promoter was used which can drive the expression of GFP in pre-osteoblasts and osteoblasts.[76] Since undifferentiated cells do not show any fluorescence, the osteoblasts can be easily identified by their strong, bright green, EYFP expression. Low EYFP expression can however, be observed in other collagen producing cells and osteoclasts.[77] Thus, use of suitable histological staining such as ALP and TRAP staining can help in identifying and deciphering the spatial distribution of various cell types involved in bone regeneration. For instance, the actively mineralizing osteoblasts show co-localized ALP activity (active osteoblasts stain red) and an additional underlying alizarin complexone label (thin red line) along with the strong EYFP expression. Osteoclasts can be identified by the low EYFP expression, along with strong TRAP positive (yellow) staining. One can also identify periosteum-like fibroblastic cells which may show low EYFP expression, but are negative for ALP, TRAP as well as AC.[76, 78]

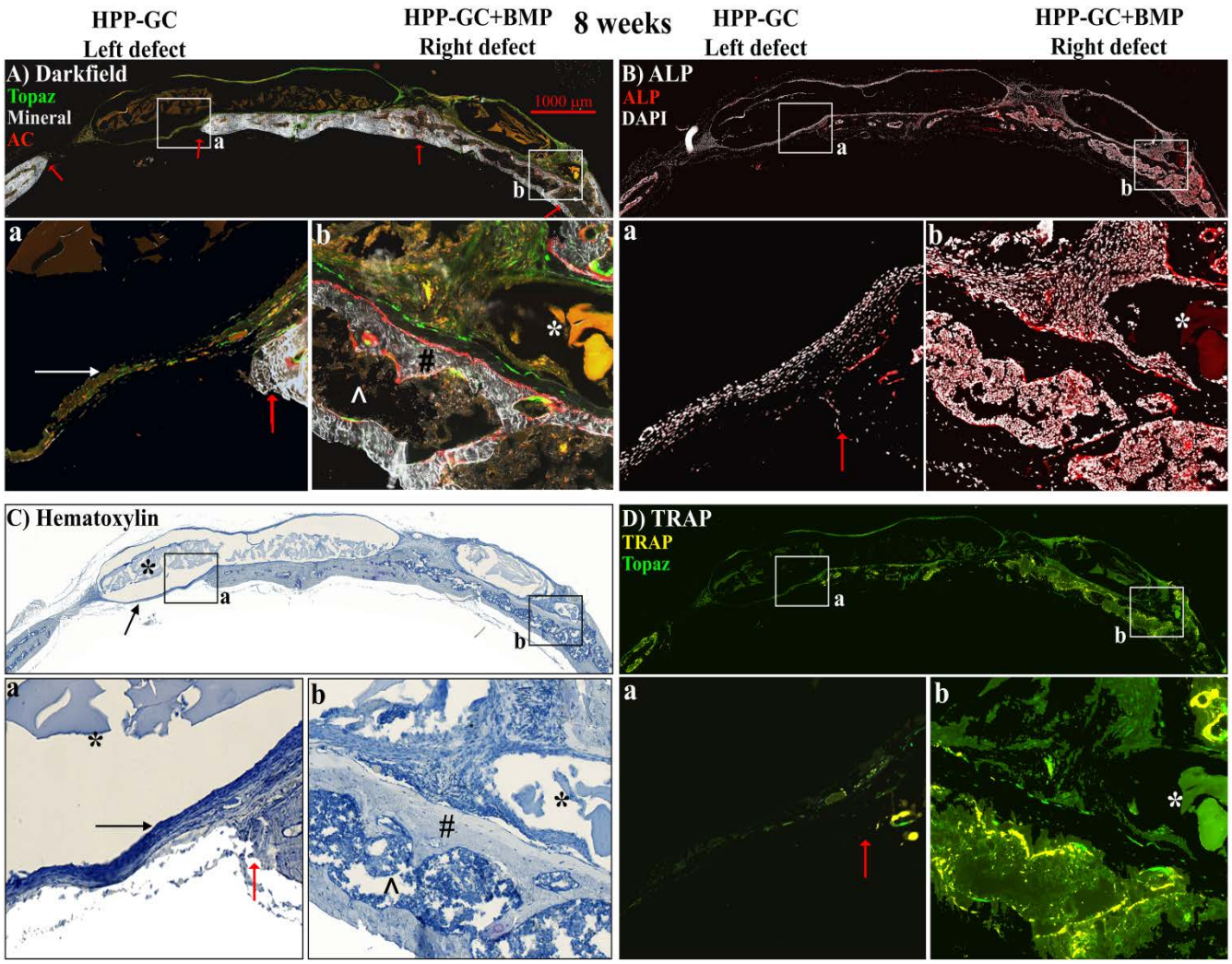

Fig. 7 Histology showing A) Darkfield, B) ALP, C) Hematoxylin and D) TRAP stained sections of the critical sized defects after 8 weeks of implantation with enzymatically cross-linked, injectable HPP-GC hydrogels with or without rhBMP-2. Full calvarial sections (scale bars: 1000 µm). Darkfield sections show EYFP reporter expression in the regenerated tissues along with alizarin complexone (AC) labeling. The defect edges are marked by red arrows. Bright, EYFP positive, green cells lined with a red mineralizing AC label are mature osteoblasts. Light green elongated cells form a periosteum-like layer at the periphery of the defects. TRAP: Bright yellow stain co-localized with low EYFP expressing cells represents TRAP positive osteoclasts. ALP: Red color indicates ALP positive cells. Cell nuclei are stained white with DAPI. (*) non-degraded gel; (#) New bone with embedded osteocytes; (^) Marrow-like matrix; (arrow) Periosteum-like fibrous layer composed of cells expressing low EYFP, but negative for AC, ALP or TRAP

Fig. 5 shows the representative photographs of isolated whole calvaria and the corresponding x-ray scans. Figs. 5A & D show the empty, critical sized parietal defects before implantation. At 4 weeks, the left defect with HPP-GC gel alone did not show any radiopaque mineralized tissue formation, whereas the right defect with HPP-GC+BMP gel showed closure of defect site with new, radiopaque tissue (Figs. 5B & E). At 8 weeks post-surgery, the defects with HPP-GC+BMP gel maintained the radio opacity, whereas the HPP-GC gel site showed complete lack of mineralized tissue (Figs. 5C & F).

Cryo-histological evaluation of the regenerated tissue was performed to understand the cellular activity and the extent of new bone formation at the defect sites. Figs. 6A-D show the representative darkfield images along with ALP, hematoxylin and TRAP stained tissue sections and the magnifications of boxed areas of the defect sites implanted with HPP-GC and HPP-GC+BMP gels, at 4 weeks post-surgery. The defect edges are marked by red arrows. The left defect with HPP-GC gel alone showed little cellular infiltration and no mineralized tissue formation at the defect site (Fig. 6A). The cells infiltrating the defect site were mostly fibroblastic in nature as evidenced from the faint green fluorescence (white arrow, Fig. 6Aa). The fact that these cells did not show any AC label, TRAP or ALP activity further confirmed that these were neither osteoblasts nor osteoclasts in nature (Figs. 6A, B & D, left defect). The data confirms the lack of osteogenic activity of HPP-GC hydrogel.

In contrast, the right defects with HPP-GC+BMP gel showed new bone formation almost completely closing the critical sized defect. High magnification darkfield images (Fig. 6Ab) of the newly formed bone showed presence of Col3.6Tpz osteoblasts (confirmed by the presence of strong EYFP expression) on the bone surface with an underlying mineralizing label (thin red line). The label signifies the incorporation of AC dye into the new bone formed within 24h of sacrifice. The ALP activity, indicated by red coloured stain in

Fig. 6Bb, was co-localized with the EYFP positive cells observed in Fig. 6Ab, implying that these were actively mineralizing osteoblasts. The sections also showed the presence of TRAP positive osteoclasts at the defect site (Fig. 6Db). Hematoxylin staining showed presence of blood vessels (depicted by circle) at the defect site (Fig. 6Cb). The new bone was surrounded with a thin periosteum-like layer composed of lightly EYFP positive fibroblastic cells (indicated by arrow in Figs. 6Ab and 6Cb). These cells however, did not show AC label, ALP or TRAP activity. The data indicates that implantation of rhBMP-2 loaded HPP-GC gel could heal a critical sized defect and lead to the formation of mineralized tissue. The regenerated tissue showed robust osteogenic activity involving actively mineralizing osteoblast cells and was undergoing remodelling as indicated by the presence of TRAP positive osteoclasts (Fig. 6Db). The 4 weeks histological sections however, showed significant hydrogel residue at the site of implantation (indicated by *).

Similar to the 4 week time point, the defects with HPP-GC gel alone did not show mineralized tissue formation, at 8 weeks (Fig. 7, left defect). The non-degraded gel was present even at 8 weeks at the defect site completely encapsulated by a thin fibrous capsule layer composed of fibroblastic cells expressing low EYFP, with no AC, ALP or TRAP activity (indicated by arrow). The defect implanted with HPP-GC+BMP gel showed complete closure of the defect site. The newly formed bone was morphologically similar to mature lamellar bone and showed presence of thin marrow-like cavity (indicated by ^), as seen in the darkfield (Fig. 7Ab) and hematoxylin stained (Fig. 7Cb) sections. High magnification images of the new bone revealed the presence of ALP positive, EYFP positive osteoblasts next to the mineralizing AC label (thin red line) along with EYFP positive osteocytes embedded in the mineralized neo-tissue (Figs. 7Ab & Bb). TRAP activity seemed to be located at the edge of the new bone towards the marrow-like cavity (Fig. 7Db).

Even though complete defect closure was observed in the right defects loaded with HPP-GC-BMP gel, non-degraded hydrogel remnants could be seen at the defect site even after 8 weeks post-surgery, indicating very slow degradation of HPP-GC gels. The in vitro and *in vivo* degradation of chitosan occurs by lysozyme mediated cleavage of N-acetyl glucosamine moieties of the polymer. The HPP-GC polymer used in the present study has a degree of acetylation (DA) of ~7% as determined by NMR (data not shown). The presence of non-degradable gel components at the defect site can therefore be attributed to the low degree of acetylation of the glycol chitosan used. The degradation rate of the chitosan gels can be increased by incorporating hydrolytically or enzymatically labile segments into the hydrogel or by simply increasing the DA of the parent polymer.[79] Ongoing studies are focused on developing HPP-GC with tunable degradation profiles to support complete gel degradation for successful regenerative approaches.[80, 81]

The complete regeneration of critical sized defects at 4 weeks, along with the formation of a mature, lamellar bone with a marrow space similar to native bone at 8 weeks observed in HPP-GC+BMP implanted defect sites, confirms the osteoinductivity of the loaded rhBMP-2. Our previous study using Healos™ as a rhBMP-2 delivery vehicle also showed good bone formation at this time point using the same BMP-2 dose.[75] However, the study showed the formation of bone at the implanted site as well as the neighbouring site in the bilateral calvarial model. Healos™ exhibits fast degradation *in vivo* and therefore presumably led to faster rhBMP-2 release thereby affecting the neighbouring site. The lack of bone formation in the neighbouring site of HPP-GC+BMP loaded site observed in the present study, compared to Healos™[75] also raises interest. Further studies are currently underway to understand whether the localized rhBMP-2 bioactivity at the defect site is due to the lack of osteoconductivity of HPP-GC gel alone or due to the enhanced *in vivo* retention of rhBMP-2 in the HPP-GC+BMP implanted site.

4. Conclusions

An injectable hydrogel was developed using enzymatic cross-linking of phenol modified glycol chitosan. The hydrogel showed fast gelation in the presence of horseradish peroxidase and hydrogen peroxide with a concentration dependent increase in its storage modulus and good *in vitro* cell viability. Low *in vitro* release of rhBMP-2 from the gel indicated potential covalent conjugation of encapsulated protein during enzymatic crosslinking. The implantation of rhBMP-2 loaded hydrogels led to complete closure of critical sized bone defects *in vivo* indicating the maintenance of rhBMP-2 bioactivity. The presence of mineralizing osteoblasts and TRAP positive osteoclasts confirmed active bone remodelling at the defect site. The results demonstrate the potential of the injectable HPP-GC gel as a localized growth factor delivery system for regenerative engineering applications.

Acknowledgements

Liping Wang is acknowledged for surgical support; Li Chen is acknowledged for histological support; Eric N. James is acknowledged for SEM analysis. This work was funded by The U.S. Army Medical Research and Materiel Command, Maryland (Contract W81WXH-10-1-0653) and stem cell grant from the state of CT (Grant # 11SCB08).

References

1. R. Censi, P. Di Martino, T. Vermonden and W. E. Hennink, *J. Control. Release*, 2012, **161**, 680-692.
2. T. R. Hoare and D. S. Kohane, *Polymer*, 2008, **49**, 1993-2007.
3. J. M. Saul and D. F. Williams, in *Principles of Regenerative Medicine, Second Edition*, eds. A. Atala, R. Lanza, J. A. Thomson and R. M. Nerem, Elsevier, 2011, DOI: 10.1016/b978-0-12-381422-7.10035-5, ch. 35, pp. 637-661.
4. A. A. Amini and L. S. Nair, *Biomed. Mater.*, 2012, **7**, 024105.
5. A. A. Amini and L. S. Nair, *J. Bioactive Compatible Polym.*, 2012, **27**, 342-345.

6. M. K. Nguyen and E. Alsberg, *Prog. Polym. Sci.*, 2014, **39**, 1235-1265.
7. M. K. Nguyen and D. S. Lee, *Macromol. Biosci.*, 2010, **10**, 563-579.
8. H. Tan, C. R. Chu, K. A. Payne and K. G. Marra, *Biomaterials*, 2009, **30**, 2499-2506.
9. H. Tan and K. G. Marra, *Materials*, 2010, **3**, 1746-1767.
10. S. V. Gohil, C. W. Hanna and L. S. Nair, in *Injectable hydrogels for regenerative engineering*, ed. L. S. Nair, Imperial College Press, London, 2015, p. In Press.
11. T. Heck, G. Faccio, M. Richter and L. Thony-Meyer, *Appl. Microbiol. Biotechnol.*, 2013, **97**, 461-475.
12. L. S. Teixeira, J. Feijen, C. A. van Blitterswijk, P. J. Dijkstra and M. Karperien, *Biomaterials*, 2012, **33**, 1281-1290.
13. A. A. Amini, H. M. Kan, Z. Cui, P. Maye and L. S. Nair, *Tissue Eng. Part A*, 2014, DOI: 10.1089/ten.TEA.2013.0506.
14. S. Sakai, T. Ashida, S. Ogino and M. Taya, *J. Microencapsul.*, 2014, **31**, 100-104.
15. S. Sakai, T. Matsuyama, K. Hirose and K. Kawakami, *Biomacromolecules*, 2010, **11**, 1370-1375.
16. K. Xu, F. Lee, S. J. Gao, J. E. Chung, H. Yano and M. Kurisawa, *J. Control. Release*, 2013, **166**, 203-210.
17. M. Kurisawa, F. Lee, L.-S. Wang and J. E. Chung, *J. Mater. Chem.*, 2010, **20**, 5371-5375.
18. P. G. Furtmuller, M. Zederbauer, W. Jantschko, J. Helm, M. Bogner, C. Jakopitsch and C. Obinger, *Arch. Biochem. Biophys.*, 2006, **445**, 199-213.
19. G. S. Zakharova, I. V. Uporov and V. I. Tishkov, *Biochemistry*, 2011, **76**, 1391-4401.
20. N. Ganesh, C. Hanna, S. V. Nair and L. S. Nair, *Int. J. Biol. Macromol.*, 2013, **55**, 289-294.
21. F. Lee, J. E. Chung and M. Kurisawa, *J. Control. Release*, 2009, **134**, 186-193.
22. S. Sakai, K. Hirose, K. Taguchi, Y. Ogushi and K. Kawakami, *Biomaterials*, 2009, **30**, 3371-3377.
23. A. Bernkop-Schnürch and S. Dünnhaupt, *Eur. J. Pharm. Biopharm.*, 2012, **81**, 463-469.
24. M. Rinaudo, *Prog. Polym. Sci.*, 2006, **31**, 603-632.
25. S. V. Gohil and L. S. Nair, in *Biomaterials Science: Processing, Properties and Applications IV*, John Wiley & Sons, Inc., 2014, DOI: 10.1002/9781118995235.ch10, pp. 95-104.
26. M. Dash, F. Chiellini, R. M. Ottenbrite and E. Chiellini, *Prog. Polym. Sci.*, 2011, **36**, 981-1014.
27. X. Liu, L. Ma, Z. Mao and C. Gao, *Adv. Polym. Sci.*, 2011, **244**, 81-127.
28. F. Li, Y. Liu, Y. Ding and Q. Xie, *Soft Matter*, 2014, **10**, 2292-2303.
29. J. H. Hamman, *Mar. Drugs*, 2010, **8**, 1305-1322.
30. A. V. Il'ina and V. P. Varlamov, *Appl. Biochem. Microbiol.*, 2005, **41**, 5-11.
31. N. Bhattarai, J. Gunn and M. Zhang, *Adv. Drug Deliv. Rev.*, 2010, **62**, 83-99.
32. M. Amidi, E. Mastrobattista, W. Jiskoot and W. E. Hennink, *Adv. Drug Deliv. Rev.*, 2010, **62**, 59-82.
33. S. Sakai, Y. Yamada, T. Zenke and K. Kawakami, *J. Mater. Chem.*, 2009, **19**, 230-235.
34. I. A. Sogias, V. V. Khutoryanskiy and A. C. Williams, *Macromol. Chem. Physic.*, 2010, **211**, 426-433.
35. R. Jin, L. S. Moreira Teixeira, P. J. Dijkstra, M. Karperien, C. A. van Blitterswijk, Z. Y. Zhong and J. Feijen, *Biomaterials*, 2009, **30**, 2544-2551.
36. R. A. A. Muzzarelli, P. Ilari and M. Petrarulo, *Int. J. Biol. Macromol.*, 1994, **16**, 177-180.
37. L. Weng, A. Romanov, J. Rooney and W. Chen, *Biomaterials*, 2008, **29**, 3905-3913.
38. D. K. Knight, S. N. Shapka and B. G. Amsden, *J. Biomed. Mater. Res. A*, 2007, **83A**, 787-798.
39. J. H. Na, S. Y. Lee, S. Lee, H. Koo, K. H. Min, S. Y. Jeong, S. H. Yuk, K. Kim and I. C. Kwon, *J. Control. Release*, 2012, **163**, 2-9.
40. A. L. Hillberg, M. Oudshoorn, J. B. Lam and K. Kathirgamanathan, *J. Biomed. Mater. Res. B Appl. Biomater.*, 2014, **00B**, 000-000.
41. Z. Li, S. Cho, I. C. Kwon, M. M. Janat-Amsbury and K. M. Huh, *Carbohydr. Polym.*, 2013, **92**, 2267-2275.
42. X. Xu, Y. Weng, L. Xu and H. Chen, *Int. J. Biol. Macromol.*, 2013, **60**, 272-276.
43. J. H. Kim, Y. S. Kim, K. Park, E. Kang, S. Lee, H. Y. Nam, K. Kim, J. H. Park, D. Y. Chi, R. W. Park, I. S. Kim, K. Choi and I. Chan Kwon, *Biomaterials*, 2008, **29**, 1920-1930.
44. H. Y. Yoon, S. Son, S. J. Lee, D. G. You, J. Y. Yhee, J. H. Park, M. Swierczewska, S. Lee, I. C. Kwon, S. H. Kim, K. Kim and M. G. Pomper, *Sci. Rep.*, 2014, **4**, 1-12.
45. C. Arakawa, R. Ng, S. Tan, S. Kim, B. Wu and M. Lee, *J. Tissue. Eng. Regener. Med.*, 2014, DOI: 10.1002/term.1896, n/a-n/a.
46. H. Park, B. Choi, J. Hu and M. Lee, *Acta Biomater.*, 2013, **9**, 4779-4786.
47. L. Cao, B. Cao, C. Lu, G. Wang, L. Yu and J. Ding, *J. Mater. Chem. B*, 2015, **3**, 1268-1280.
48. N. C. Veitch, *Phytochemistry*, 2004, **65**, 249-259.
49. Y. Lee, J. W. Bae, D. H. Oh, K. M. Park, Y. W. Chun, H.-J. Sung and K. D. Park, *J. Mater. Chem. B*, 2013, **1**, 2407-2414.
50. K. M. Park, K. S. Ko, Y. K. Joung, H. Shin and K. D. Park, *J. Mater. Chem.*, 2011, **21**, 13180-13187.
51. S. V. Madihally and H. W. Matthew, *Biomaterials*, 1999, **20**, 1133-1142.
52. C. Ding, L. Zhao, F. Liu, J. Cheng, J. Gu, S. Dan, C. Liu, X. Qu and Z. Yang, *Biomacromolecules*, 2010, **11**, 1043-1051.
53. L.-S. Wang, C. Du, J. E. Chung and M. Kurisawa, *Acta Biomater.*, 2012, **8**, 1826-1837.
54. S. Sakai, Y. Ogushi and K. Kawakami, *Acta Biomater.*, 2009, **5**, 554-559.
55. L.-S. Wang, J. Boulaire, P. P. Y. Chan, J. E. Chung and M. Kurisawa, *Biomaterials*, 2010, **31**, 8608-8616.
56. J. Wu, W. Wei, L. Y. Wang, Z. G. Su and G. H. Ma, *Biomaterials*, 2007, **28**, 2220-2232.
57. Z. M. Wu, X. G. Zhang, C. Zheng, C. X. Li, S. M. Zhang, R. N. Dong and D. M. Yu, *Eur. J. Pharm. Sci.*, 2009, **37**, 198-206.
58. I.-H. Bae, B.-C. Jeong, M.-S. Kook, S.-H. Kim and J.-T. Koh, *Biomed. Res. Int.*, 2013, **2013**, 1-10.
59. F. Lee, J. E. Chung and M. Kurisawa, *Soft Matter*, 2008, **4**, 880-887.
60. H. P. Hsu, J. M. Zanella, S. M. Peckham and M. Spector, *J Orthop Res*, 2006, **24**, 1660-1669.
61. M. Geiger, R. H. Li and W. Friess, *Adv. Drug Deliv. Rev.*, 2003, **55**, 1613-1629.
62. W. Friess, H. Uludag, S. Foskett, R. Biron and C. Sargeant, *Int. J. Pharm.*, 1999, **185**, 51-60.
63. G. Bhakta, Z. X. H. Lim, B. Rai, T. Lin, J. H. Hui, G. D. Prestwich, A. J. van Wijnen, V. Nurcombe and S. M. Cool, *Acta Biomater.*, 2013, **9**, 9098-9106.
64. M. V. Burks and L. S. Nair, *J. Long Term Eff. Med. Implants*, 2010, **20**, 277-293.
65. E. J. Carragee, E. L. Hurwitz and B. K. Weiner, *Spine J.*, 2011, **11**, 471-491.
66. M. Kisiel, A. S. Klar, M. Ventura, J. Buijs, M.-K. Mafina, S. M. Cool and J. Hilborn, *PloS one*, 2013, **8**, e78551.
67. H. Zhang, F. Migneco, C. Y. Lin and S. J. Hollister, *Tissue Eng. Part A*, 2010, **16**, 3441-3448.
68. J. Kang, S. Tada, T. Kitajima, T. I. Son, T. Aigaki and Y. Ito, *Biomed. Res. Int.*, 2013, **2013**, 1-6.
69. K. Lee, E. A. Silva and D. J. Mooney, *J. Royal Soc. Interf.*, 2011, **8**, 153-170.
70. M. Geiger, R. H. Li and W. Friess, *Advanced drug delivery reviews*, 2003, **55**, 1613-1629.
71. A. R. Poynton and J. M. Lane, *Spine*, 2002, **27**, S40-48.

72. R. Budiraharjo, K. G. Neoh and E.-T. Kang, *J. Biomater. Sci. Polym. Ed.*, 2013, **24**, 645-662.
73. C. M. Madl, M. Mehta, G. N. Duda, S. C. Heilshorn and D. J. Mooney, *Biomacromolecules*, 2014, **15**, 445-455.
74. K. Minamihata, M. Goto and N. Kamiya, *Bioconjug Chem*, 2011, **22**, 74-81.
75. S. V. Gohil, D. J. Adams, P. Maye, D. W. Rowe and L. S. Nair, *J. Biomed. Mater. Res. A*, 2014, **102**, 4568-4580.
76. I. Kalajzic, Z. Kalajzic, M. Kaliterna, G. Gronowicz, S. H. Clark, A. C. Lichtler and D. Rowe, *J. Bone Miner. Res.*, 2002, **17**, 15-25.
77. I. Boban, C. Jacquin, K. Prior, T. Barisic-Dujmovic, P. Maye, S. H. Clark and H. L. Aguila, *Bone*, 2006, **39**, 1302-1312.
78. X. Jiang, Z. Kalajzic, P. Maye, A. Braut, J. Bellizzi, M. Mina and D. W. Rowe, *J. Histochem. Cytochem.*, 2005, **53**, 593-602.
79. G. D. Nicodemus and S. J. Bryant, *Tissue Eng. Part B Rev.*, 2008, **14**, 149-165.
80. S. V. Gohil, K. R. Bagshaw, D. W. Rowe and L. S. Nair, Society for Biomaterials Annual Meeting and Exposition, Denver, Colorado, 2014.
81. S. V. Gohil, A. Padmanabhan and L. S. Nair, Society for Biomaterials Annual Meeting and Exposition, Charlotte, North Carolina, 2015.

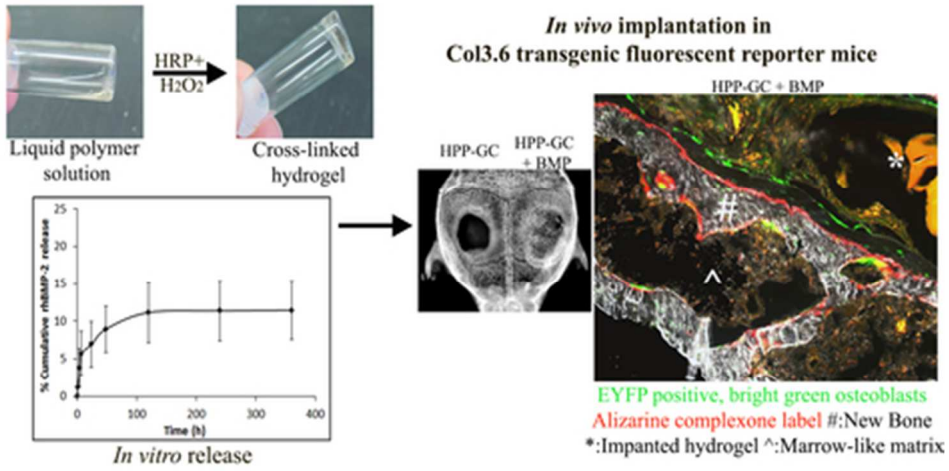

An injectable, enzymatically crosslinkable glycol chitosan hydrogel was developed and evaluated for localized growth factor delivery
39x19mm (300 x 300 DPI)